Turbulent tension distribution in turbulent boundary layer on permeable porous plate

Vlassov D.
Universidade Federal do Paraná
vlassov@demec.ufpr.br,

Vargas J. V. C.
Universidade Federal do Paraná
jvargas@demec.ufpr.br.

Abstract. *In this paper the results of an experimental test on turbulent boundary layer on a plate with air insufflation through permeable porous wall are presented. Tests were performed in an aerodynamic tunnel varying the insufflation rate within the range of 0 to 2.5% of the air flow velocity in the tunnel, using thermo anemometers of constant temperature. It has been determined that the insufflation increases the boundary layer thickness and strongly transforms the boundary layer inner part and turbulent nucleus, while the outer part remains undeformed. An increase in insufflation causes an abrupt viscous tension decrease, also decreasing the superficial friction. Thick boundary layers (up to 120 mm) allowed a deep analysis of Reynolds' turbulent tensions. It has been revealed an universal distribution of turbulent tension in the turbulent layer which is independent of insufflation velocity. It has been established for the turbulent characteristics that the determining coordinate is the relative longitudinal velocity, not the distance from the wall. With a turbulent tension database obtained from turbulent tensions direct measurements, it has been proposed a flow model for boundary layer on a permeable porous plate. It has been demonstrated that in high insufflation conditions the longitudinal velocity profile in the boundary layer becomes equal to the velocity profile in plane jet.*

Key words: ***t****urbulent boundary layer, Reynolds' turbulent tensions, porous material, air insufflation, thermoanemometer.*

1. Introduction

The insufflation through permeable walls aiming to control the boundary layer development has been dragging attention from scientists and engineers. Due to its high efficiency, this method is used to solve practical problems. Some of these problems might be cited:
- thermal protection ("transpiration" method) of surface exposed to high amounts of enthalpy flows (gas turbine blades, combustion chamber walls and other rocket engine parts, airplate wings or frames and other flying machines, etc.);
- Superficial friction decrease of airplanes, ships, wings and equipments immersed in water and lift increase of aircraft etc.

In case of thermal protection, the conduction of a secondary flow through permeable wall allows the wall temperature control at a specific level to keep it working safely. The economic performance of this method depends on the way the secondary flow is supplied to the surface. The most economic method is the one in which the secondary flow is supplied through a porous wall.

Even if one takes into account the simplest conditions (isothermal boundary layer, no longitudinal pressure gradient, uniform insufflation, etc.) the turbulent boundary layer equations system is not closed due to lack of knowledge about Reynolds' turbulent tensions. To close the system of equations several hypothesis are considered that generally set a correlation between the Reynolds' turbulent tensions and average longitudinal velocity on the boundary layer. However, among hundreds of hypothesis it has not been found a universal one that would fit to the whole boundary layer and this is the reason experimental research on turbulent boundary layer properties is indispensable. Contemporary measurement methods of Reynolds' turbulent tension on the boundary layer (laser anemometers and hot wire) have faced difficulties related to boundary layers low thicknesses, high velocity gradients near wall and wall presence influence.

Turbulent tensions exert a main influence on the average velocity profile in the boundary layer formation. Measurements data taken in the boundary layer on a impermeable sheet support the existence of a turbulent tension maximum near the wall. The decrease of turbulent tension on the boundary layer outer part was studied by several authors, but their "behaviour" on the left of the maximum is yet to be defined. However, it is known fluid insufflation in the boundary layer, through permeable wall reduces abruptly the velocity gradient near the wall and leads to an enlargement of the low velocity values zone, which allows the researcher to study profoundly the essence of formation and development of turbulent tensions in the vicinities of the wall.

The development of a theory on boundary layer control using fluid insufflation through porous walls, the elaboration of precise mathematical models, and the numerical simulation of flows in the turbulent boundary layer require profound knowledge of energy and mass turbulent transport phenomena. The present paper objective is to study experimentally turbulent boundary layer transformation patterns on porous planes.

2. Experimental model, flow parameter and equipments

The model is a plate of 2.53 m total length and 0.4 m width. The plate consisted of a front impermeable segment of 1 m, a porous permeable segment of 1.03 m and a rear segment of 0.5 m. The front segment length was designed to assure a developed turbulent boundary layer in the beginning of the permeable segment, Re ≈ $6.5 \cdot 10^5$, and the rear segment length was calculated to avoid the influence of separation of the boundary layer on the porous segment.

The porous sheet was manufactured by a hot forming process in vacuum media using stainless steel meshes. The porous sheet thickness was 7.75 mm, the porosity 11.8 %. The porous diameter average value was 15 μ m. Air insufflation was measured by means of a micro flow rate meter based on a thermoanemometer. Air insufflation variation was within 10 %. In the middle of the plate, where measurements were taken, it was within 5 %.

The experimental research was performed in a subsonic aerodynamic tunnel, equipped with an Eiffel chamber. The test chamber consisted of a regular octagon with distances among walls of 800 mm and length of 1750 mm. The aerodynamic tunnel was instrumented by an automatic air velocity control system that has a continuous current starter engine with reaction coupling. The performance of this system allowed stabilization of the tunnel fan speed and, consequently air speed. The air flow parameters were as follows: air free stream velocity U_∞=10 m/s (± 0.5 %); turbulence rate at nozzle exit 0.5 %; at diffuser entrance 0.7 %; air temperature ~20°C; pressure gradient in the test chamber was $\frac{dp}{dx} \cong 0$.

The insufflated air velocity through the porous wall had seven discrete values V_w = 0 (no insufflation); 0.05; 0.1; 0.142, 0.18; 0.212 and 0.243 m/s, where: V_w - normal velocity component, the subscript w indicates a parameter value at the wall.

To move the transducers in the boundary layer a special coordinating mechanism with remote control was used. The mechanism had two degrees of freedom for vertical translation (along the vertical axis y and around it). The linear and angular precision was ± 0.01 mm and ± 0.1°, respectively.

The transducer distance from the wall to the plate was measured with an optic cathetometer with precision of 0.001 mm and focal distance of 650 mm.

The following equipments were also used:

- 4 hot wire anemometers made in Denmark;
- 2 current linearizers , to obtain a thermoanemometer linear output;
- 1 analogic correlating device, and
- 1 magnetic recorder with 20 channels of frequency modulation.

The transducer or thermoanemometer sensor had a wire with a diameter of 5 μm and a length of 1.2 mm. It was made from tungsten and covered with a platinum layer to avoid corrosion.

3. Methodology

3.1. Average velocity components determination

In the boundary layer on the porous permeable plate, with insufflation, an accentuated curvature in the streamlines is observed. Right on the wall, the velocity vector $\vec{W}_w$ is driven by the wall surface normal vector and is numerically equal to the insufflation velocity V_w, because at the wall $W_w = V_w$. As the distance from the wall increases the streamlines bend and the angle between the velocity vector and the wall, φ, diminishes. At the external edge of the boundary layer, the velocity vertical component is null, $V_\infty = 0$ and the velocity becomes equal to the free stream velocity, $W = U_\infty$ (the infinity subscript is used to indicate a parameter outside the boundary layer). To calculate the velocity longitudinal and vertical components $U(y)$ and $V(y)$ is therefore necessary to know $\vec{W}(y)$.

To decompose the velocity vector into components U and V a special methodology was devised (Vlassov, 1975, 2002). The phenomenon of heat transfer variation between the thermoanemometer wire and the air as a function of the wire position with respect to the velocity vector $\vec{W}$ was used. The thermoanemometer wire was calibrated in a special air tunnel as a function of the velocity variation and the angle φ. Based on the calibration results, a graph was drawn, $E = f(W, \varphi)$, where: E - thermoanemometer output (tension), in Volts.

During the test, the sensor was mounted at a point in the boundary layer at two positions (see Fig. 1): position a) perpendicular to the sheet longitudinal axis x; position b) parallel to the same axis. Two values from the thermoanemometer were recorded $E_\perp$ e $E_{//}$. The values of W and φ were determined using the calibration chart.

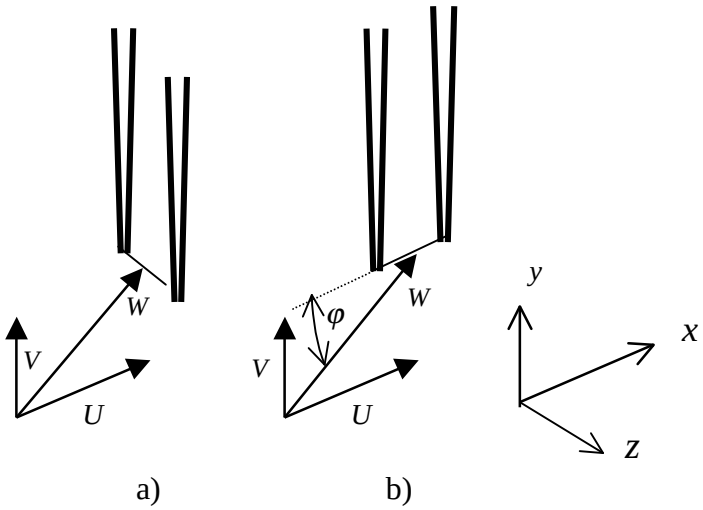

Figure 1. Thermoanemometer transducer position in the boundary layer.

The velocity vector components were calculated as $U = W\cos\varphi$ e $V = W \cdot sen\varphi$.

3.2. Turbulent tensions determination

The total tangential tension (shear) in the boundary layer consists of viscous and turbulent tensions

$$\tau = \tau_\upsilon + \tau_\tau = \mu \frac{dU}{dy} - \rho\overline{u'\upsilon'}, \tag{1}$$

where: τ - total tangential tension;
τ_υ - viscous tangential tension;
τ_t - turbulent tangential tension;
μ - dynamic viscosity;
ρ - density, and
$\overline{u'\upsilon'}$ - mean value of the instantaneous product of the longitudinal and vertical turbulent components (corresponding to) of velocity.

The viscous tensions τ_υ are determined from the average longitudinal velocity profile U in the boundary layer and the turbulent tensions τ_t are a result of the inertial interaction and non-linear velocity pulsations.

A well established method and tested in practice, of turbulent tensions determination is based on the following formula [Hinze, 1959]

$$\tau_t = -\rho\overline{u'\upsilon'} = \rho R_{u'\upsilon'} \sqrt{\overline{u'^2}} \sqrt{\overline{\upsilon'^2}}, \tag{2}$$

where: $\sqrt{\overline{u'^2}}$ - intensity (dispersion) of the turbulent longitudinal component;
$\sqrt{\overline{\upsilon'^2}}$ - intensity (dispersion) of the turbulent vertical component, and
$R_{u'\upsilon'}$ - correlation coefficient.

Another well established method of velocity turbulent components measurement is based on the use of two themoanemometer and one thermoanemometric transducer in X (see Fig. 2) (Hinze, 1959).

During the measurement of velocity turbulent components u' e υ', it is generally considered that the wires should be on a vertical plate $x0y$ and the transducer axis in X should coincide with the longitudinal velocity component. In this case, the linearized thermoanemometer floating outputs are the following:

$$e_1' = \frac{\beta}{\sqrt{2}}(u' + \upsilon') \quad \text{e} \quad e_2' = \frac{\beta}{\sqrt{2}}(u' - \upsilon') \tag{3}$$

where: e_1' e e_2' - linearized thermoanemometer floating outputs (tension), in Volts;
β - linearization coefficients.

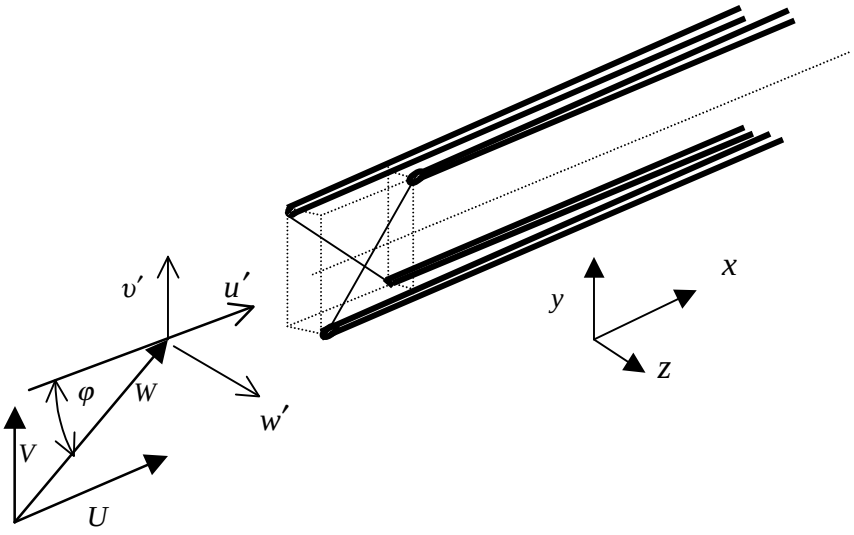

Figure 2. Thermoanemometer transducer position in X in the boundary layer.

The sum of $e_1' + e_2'$ is proportional to u', the difference is proportional to υ'. The values of $\sqrt{\overline{u'^2}}$ and $\sqrt{\overline{\upsilon'^2}}$ were determined after separation of the components.

The turbulent tensions were determinated by means of Eq. (2). In the boundary layer, the correlation coefficient varied within the range $\approx$(-0,42)< $R_{u'\upsilon'} \leq 0$. On the wall, the velocity pulsations are null and the correlation coefficient equals to zero, $R_{u'\upsilon'}$=0. While moving farther from the wall, the correlation coefficient decreases to the minimum value – 0,42. At the boundary layer external edge, it equals zero. The negative sign of the correlation coefficient indicates that the longitudinal and vertical instant means values of the turbulent components vary contrarily. The correlation coefficient measurements showed that it varies only as a function of the relative velocity $\overline{U} = \frac{U}{U_\infty}$. The insufflation intensity had a little influence on the correlation coefficient.

An evaluation of the angle φ influence on the measured turbulence parameters was conducted. The calculations showed that for the angle $\varphi = 0$, in Eq. (3) the first equation is correct within a 2 % margin and the second equation is also correct within a 9 % margin. The precision of the first equation increases with increasing φ angles and the precision of the second equation increases with an angle increasing and then decreases, but within the range $0 < \varphi < 35°$, it is not over a 9 % margin.

Another measurement method of turbulent tensions is to obtain directly the electric sign proportional to $u' \times \upsilon' = u'\upsilon'$ and in the determination of the average value of $\overline{u'\upsilon'}$. For that, Eq. (3) was raised to the square power and the difference $e_1^2 - e_2^2 = 4\frac{\beta_l^2}{2} u'\upsilon'$ was determined.

The instantaneous product average value was determined from the readings of a continuous current voltmeter.

$$\overline{u'\upsilon'} = \frac{\overline{e_1^2 - e_2^2}}{2\beta} \tag{4}$$

In the present paper both turbulent tensions determination methods were used, by means of Eq. (3) and (4). Both methods showed similar results. The second one is preferential because it does not require a coordinating mechanism to evaluate the correlation coefficient.

5. Turbulent tensions

High boundary layer thicknesses induced by insufflation allowed for deeper turbulent tensions instrumental investigations. Traditionally turbulent tensions distribution graphs are presented as a function of the vertical coordinate,

for $\overline{u'v'} = f(\bar{y})$, where $\bar{y} = \frac{y}{\delta}$. In these coordinates, right on the wall and outside the boundary layer, the turbulent tensions are null. In non-insufflation conditions, the turbulent tensions maximum is acute and is located near the wall, in the boundary layer turbulent nucleus. The insufflation rise increases the turbulent tensions maximum, and moving it away from the wall, following the boundary layer turbulent nucleus. Besides, the turbulent tensions maximum becomes smooth. The turbulent tensions maximum values treatment as a function of the insufflation parameter resulted in the following equation:

$$\frac{\overline{u'v'}_{max}}{\overline{u'v'}_{max\,0}} = 1 + 3.86 \cdot \bar{V}_W^{1/3}, \tag{5}$$

where: $\overline{u'v'}_{max}$ - turbulent tensions maximum value in case of insufflation, and

$\overline{u'v'}_{max\,0}$ - non insufflation turbulent tensions maximum value.

In experimental conditions, at the highest insufflation value $\bar{V}_W = 0.0243$, the turbulent tensions values increased more than twice.

The analysis of the measured data of the turbulent characteristics of the boundary layer, particularly the relative turbulent tensions $\bar{\tau}_t = \frac{\overline{u'v'}}{\overline{u'v'}_{max}}$, showed that in their case, the more appropriate coordinate is the relative velocity $\bar{U}$, instead of $\bar{y}$. Figure 3 shows the $\bar{\tau}_t = f(\bar{U})$ distribution, which has a universal shape for all insufflation intensities.

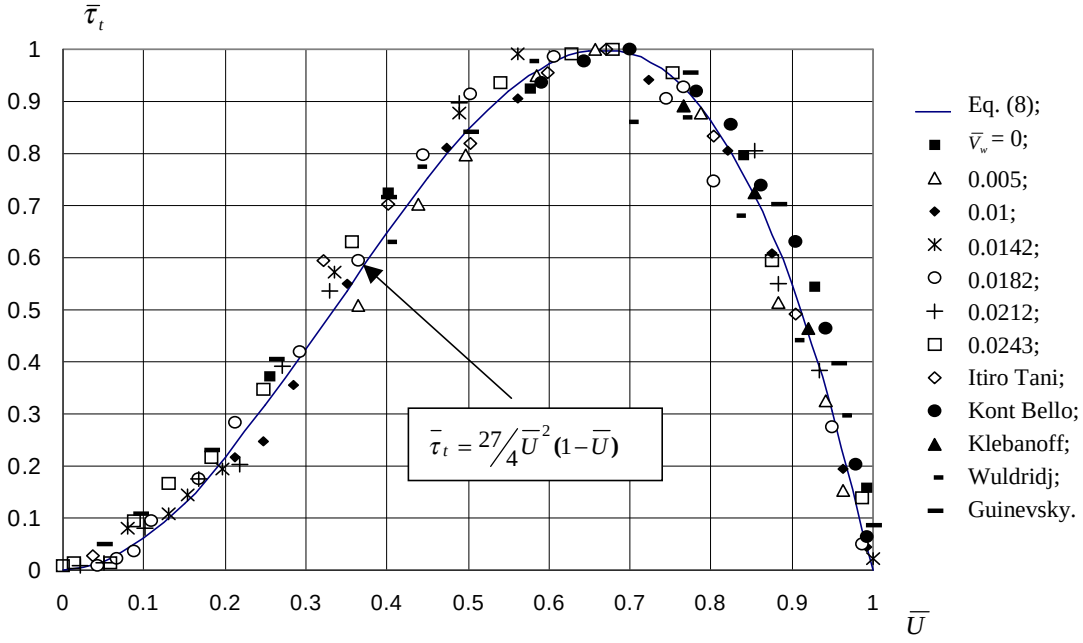

Figure 3. Relative turbulent tensions distribution in the boundary layer as a function of relative longitudinal velocity.

The relative turbulent tensions maximum corresponds to $\bar{U} = 2/3$. In the same figure several other data are placed: Itiro Tani's (1969) – permeable porous sheet; Kont Bello's (1968) – plane channel; Klebanoff's (1968) – impermeable sheet and Wuldridj's (1966) – permeable sheet.

In this paper, in the non-insufflated boundary layer it was not possible to measure turbulent tensions near the wall where $\bar{U}$ < 0,6. However, under insufflation, a possibility of measuring lower velocitys appeared. It is important to note that with an insufflation increase, the turbulent tensions values measured kept the general tendency until longitudinal velocitys close to zero. This discovery may be used to propose new semi-empiric methods of turbulent boundary layer calculation and also for numerical simulations.

The tendency curve was adjusted from the data in the form of a 4th polynomial as follows

$$\bar{\tau}_t = \frac{\overline{u'v'}}{\overline{u'v'}_{max}} = f(\bar{U}) = a + b\bar{U} + c\bar{U}^2 + d\bar{U}^3 + e\bar{U}^4 \tag{6}$$

To find the coefficients a, b, c, d and the tendency curve, the following boundary conditions were used:

$$\left.\begin{array}{lll} \text{for } \overline{U} = 0, & f(\overline{U}) = 0 \text{ e } & f'(\overline{U}) = 0; \\ \text{for } \overline{U} = 1, & f(\overline{U}) = 0; & \\ \text{for } \overline{U} = 2/3, & f(\overline{U}) = 1 \text{ e } & f'(\overline{U}) = 0. \end{array}\right\} \quad (7)$$

Under such conditions, Eq. (6) becomes

$$\overline{\tau}_t = f(\overline{U}) = 27/4\,\overline{U}^2(1-\overline{U}) \quad (8)$$

The tendency curve shows excellent agreement with the measured data.

6. Turbulent boundary layer on permeable porous plate formation patterns

The analysis of the experimental data on the turbulent layer velocity distribution reveals the fact that the flow outside the boundary layer does not depend on the phenomena occurred on the wall and develops according to its own rules. It is interesting to match the external parts of the longitudinal velocity profiles. This is possible to be done by building the velocity profiles not from the wall, as shown in Fig. 3, but from the profiles external parts, as shown in Fig. 4.

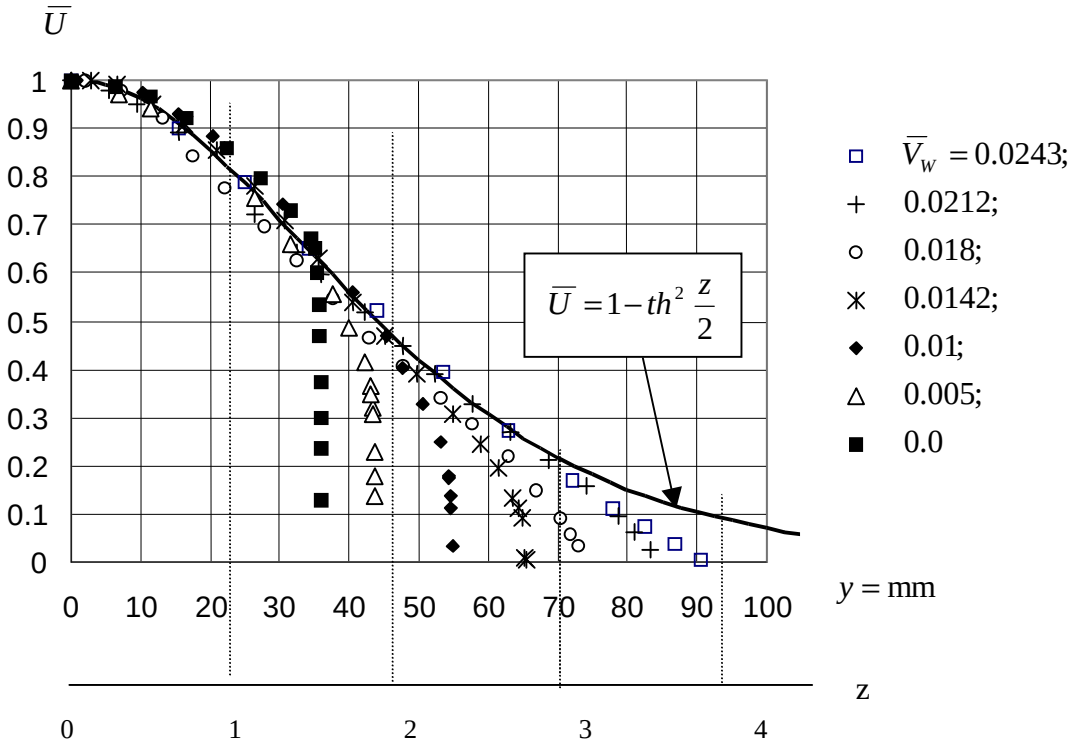

Figure 4 Longitudinal velocity profiles built with boundary layer external edge origin, x=700 mm

One might observe all profiles are coincident within the longitudinal relative velocity range $2/3 < \overline{U} < 1$. This range of the velocity profile corresponds to the turbulent tensions descending interval. Increasing the insufflation, the velocity profiles become more coincident in the highest $\overline{U}$ variation range. It is logic to suppose there is an asymptotic profile that corresponds to the highest value of insufflation parameter. This profile can be determined under the supposition that with an insufflation increasing the laminar tensions become negligible in presence of turbulent tensions.

This assumption has a solid basis. In Figure 5, it is shown a comparison between viscous and turbulent tensions for several insufflation parameters.

On the wall surface with no insufflation, the viscous tensions $\tau_\upsilon = \mu \frac{dU}{dy}$ have a maximum value and the turbulent tensions $\tau_t = -\rho\overline{u'\upsilon'}_{\max}$ are at a minimum. For that reason, the correspondent curve $\overline{V}_w = 0$ abruptly goes up. The

insufflation decreases the longitudinal velocity gradient in the boundary layer and because of that, the ratio $\frac{\tau_v}{\tau_t}$ value also decreases and for $\overline{U} > 2/3$ the viscous tensions are lower than 3 % of the maximum turbulent tensions. An insufflation increase decreases abruptly the viscous tensions and when the insufflation parameter is $\overline{V}_w > 0.018$ they do not reach, even on the wall, 1 % of the maximum turbulent tensions. These observations validate the former assumption.

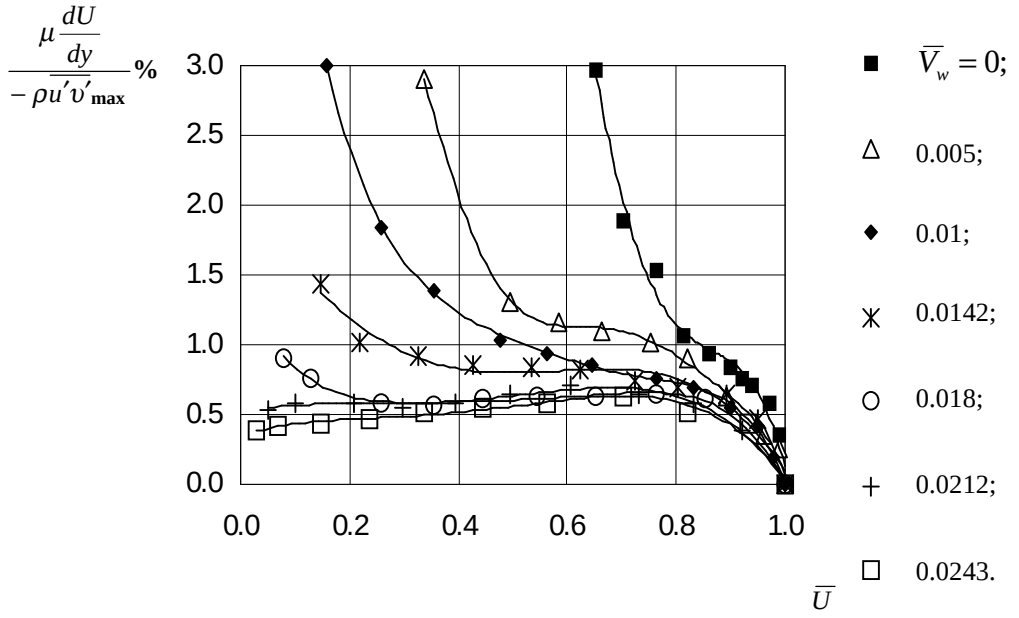

Figure 5. Ratio between viscous and turbulent tensions as a function of insufflation.

To find out the velocity profile analytic expression for high insufflation parameter values one may use the Prandtl's hypothesis for turbulent tensions:

$$\tau_t = \rho \ell^2 \left(\frac{dU}{dy} \right)^2, \tag{9}$$

where: ℓ - mixed length.

Using the turbulent tensions distributions of Eq. (8) and equalizing the right sides of Eq. (8) e (9), it is obtained

$$\left(\frac{d\overline{U}}{d\overline{y}} \right)^2 = A\overline{U}^2 \left(1 - \overline{U} \right), \tag{10}$$

where: $A = \frac{27}{4} \frac{\delta^2}{\ell^2} \frac{\tau_{t\,max}}{\rho U_\infty^2}$, constant.

After integration, it follows

$$\overline{U} = 1 - th^2 \frac{z}{2}, \tag{11}$$

where: $z = \sqrt{A} \left(1 - \overline{y} \right)$, argument.

The graphic representation of Eq. (10) is also shown in Fig. 4. Equation (10) is known, in the gas dynamics science, as the velocity profile for plane jets. From this analysis it results that under an increase of the insufflation rate in the

turbulent boundary layer, the longitudinal velocity profile tends asymptotically to the plane jet velocity profile. This result was confirmed based on experimental data from turbulent plane jet measurements (Guinevsky A S., 1969).

6. Conclusion

In the present work, a universal correlation between relative turbulent tensions and relative longitudinal velocity was established. Based on this correlation, it has been presented a flow model for turbulent boundary layer on permeable porous plane and demonstrated that under high insufflation intensities, the velocity profile approaches the velocity profile in plane jet flow.

7. Bibliographic References.

Guinevsky A S., 1969, “Teoria de Jatos Turbulentos”, Construção de Máquinas, Moscou.

Hinze J.O., 1959, ”Turbulence (An introduction to its mechanism and theory)”, McGRAW-HILL B.C., NY,

Itiro Tani, 1969, “Computation of Turbulent Boundary Layers”, V.1, Conference Proceedings California.

Kont Bello G., 1968, Escoamento Turbulento em Canal com Paredes Paralelas”, Mir, Moscou.

Klebanoff 1968, P. S., “Characteristics of Turbulent Boundary Layers with zero Pressure Gradient”, NACA Report, 1247.

Vlassov D., 2002, “Atrito superficial sobre plano poroso permeável”, II Congresso Nacional de Engenharia Mecânica, João Pessoa – PB, Brazil.

Vlassov D., Polyaev V., 1975, “Using Hot-wire Probes for Investigation of Flow in the Boundary Layer Along a Permeable Surface”, DISA Information, Measurement and Analysis, N 18, pp. 11-14.

Wuldridj Mucci, 1966, “Técnica de Foguete e Cosmonâutica”, pp. 159-168.

8. Copyright warning